IJIREEICE ISSN (O) 2321-2004, ISSN (P) 2321-5526

International Journal of Innovative Research in Electrical, Electronics, Instrumentation and Control Engineering

Impact Factor 8.021 ⁜ Peer-reviewed & Refereed journal ⁜ Vol. 13, Issue 3, March 2025

DOI: 10.17148/IJIREEICE.2025.13372

Design and Implementation of a High-Speed Charging Architecture for Intelligent Solar-Powered Battery Charging and Swapping Stations

Onyeyili T.I[1], Oranugo C.O[2], Ugwuanyi Gilbert[3]

Department of Electronic and Computer Engineering, Nnamdi Azikiwe University, Awka[1-3]

Abstract: The rapid expansion of electric vehicle (EV) adoption necessitates advanced, user-oriented charging infrastructures capable of accommodating variable daily demand. Conventional plug-in charging methods often result in prolonged vehicle downtime, prompting the exploration of battery-swapping stations as a practical alternative. This study presents the design and implementation of a high-speed solar charging architecture tailored for smart battery-swap stations. The system integrates a fast Maximum Power Point Tracking (MPPT) DC-DC solar charge controller engineered to recharge lithium-ion battery packs from 0 % to 100 % within approximately 2–3 hours. Key design objectives include maximizing charging efficiency, prolonging battery lifespan, and incorporating intelligent thermal-management strategies. Performance optimization is achieved through an advanced control algorithm executed on an ESP32 microcontroller, leveraging its high-frequency processing capability, dedicated analog-to-digital conversion for precise switching control, and Wi-Fi connectivity for real-time parameter adjustment. Experimental validation confirms the enhanced reliability and efficiency of the proposed fast-charging system, positioning it as a robust solution for next-generation smart solar charge/swap infrastructures.

Keywords: Fast Charging · Smart Solar Station · Battery Swapping · Power Electronics · Renewable Energy Integration

I. BACKGROUND OF STUDY

The accelerating growth of the electric vehicle (EV) industry is driven primarily by the need to mitigate greenhouse gas emissions and combat climate change. Projections indicate that the African EV market could reach a valuation of approximately USD 21.4 billion by 2027. Achieving this target requires the deployment of efficient, cost-effective charging infrastructures that function much like conventional fuel stations but are enhanced with advanced control algorithms (Narasipuram & Mopidevi, 2021). Solar energy has emerged as a compelling renewable power source for EV charging stations, offering both environmental and economic advantages. Integrating solar power into charging networks aligns with global strategies to reduce carbon footprints and promote sustainable energy use. Developing high-speed charging systems for intelligent solar charge/swap stations, however, demands the fusion of renewable generation, sophisticated energy-management frameworks, and state-of-the-art power-electronics technologies. These components collectively address the variability of solar supply while improving charging efficiency and long-term sustainability. Fast-charging stations (FCS) can exploit solar photovoltaic (PV) generation supported by energy-storage systems (ESS) to ensure uninterrupted high-power delivery, even during periods of limited sunlight (Yu & Shanshan, 2017). The synergy between solar PV and ESS reduces dependence on the utility grid while enabling rapid vehicle turnaround times (Nair & Fernandes, 2018). In this context, the present research focuses on designing and implementing a fast-charging architecture for a smart, solar-powered charge/swap station tailored to e-rickshaw operations. By utilizing solar energy as the primary source, the system aims to lower operational costs, enhance sustainability, and integrate advanced fast-charging solutions that streamline both charging and battery-swapping processes—minimizing downtime and overcoming the limitations of conventional EV charging infrastructure.

II. LITERATURE REVIEW

Gupta et al. (2020) introduced a Power Quality Charging System (PFCC) tailored for E-rickshaws that integrates rooftop solar photovoltaic (PV) support. The PFCC employs a discontinuous inductor current mode (DICM) to maintain voltage-follower operation across diverse supply and load conditions. Leveraging the continuous input and output currents of a Ćuk converter, the system extracts maximum power from the PV array while minimizing ripple. This configuration reduces magnetic component size, lowers the number of sensing devices and overall component count, ensures isolation

IJIREEICE ISSN (O) 2321-2004, ISSN (P) 2321-5526

International Journal of Innovative Research in Electrical, Electronics, Instrumentation and Control Engineering

Impact Factor 8.021 ⁜ Peer-reviewed & Refereed journal ⁜ Vol. 13, Issue 3, March 2025

DOI: 10.17148/IJIREEICE.2025.13372

between the supply and the battery, and enables uninterrupted charging even during grid outages. Performance and control strategies were validated in MATLAB/Simulink under varying supply voltages, loading conditions, and solar irradiation levels.

Building on the need for rapid EV charging where grid capacity is limited, Assadi et al. (2023) proposed a modular multiport linear fast charger (LFC) that replaces traditional battery-assisted DC fast chargers (BA-DCFCs). The LFC integrates a reconfigurable battery energy storage system (rBESS), a digitally controlled bidirectional linear regulator (LR), and a contactor matrix. This linear regulator significantly improves station efficiency while mitigating size, cooling, and high-frequency switching issues common in isolated DC–DC converters. Compared with conventional isolated DC–DC designs, the LFC achieves an 83.6 % reduction in losses for equivalent EV charging power and demonstrates 28 % lower daily losses, with an average efficiency of 93.4 %. Extensive transient simulations and hardware-in-the-loop experiments with a custom LR and series-connected battery modules validated the system's performance and redundancy at the station, BESS, and LR levels, while enabling active state-of-charge and health balancing without additional switched-mode converters.

Addressing grid stability challenges, Arya and Das (2023) analyzed the high-power demand of fast-charging stations—typically 80–240 kW for 30-minute charging sessions—and their potential to cause voltage fluctuations. They proposed a renewable-integrated DC microgrid that employs a multi-step constant-current fast-charging strategy. The system supports both solar PV generation and vehicle-to-grid (V2G) power transfer during low-demand or peak-demand periods. Using a coulomb-counting state-of-charge estimation method, simulations demonstrated that this approach effectively mitigates grid disturbances.

Similarly, Ayyadi et al. (2024) highlighted the importance of pairing electric vehicles with renewable sources to foster sustainable urban transport while counteracting the intermittency of renewable generation. They presented a cost-optimized energy management system (EMS) for a solar-PV-assisted fast-charging station that incorporates energy storage and dynamic electricity pricing. The EMS, formulated as a mixed-integer linear programming (MILP) model and solved with IBM ILOG CPLEX, manages power flows among the grid, PV system, ESS, EV chargers, and building loads. Case studies in Auckland, New Zealand, confirm that integrating solar PV and ESS in fast-charging stations is both technically feasible and economically viable, offering a replicable framework for global deployment.

III. SYSTEM DESIGN

Solar photovoltaic (PV) modules produce direct current (DC) electricity whose voltage and current vary with solar irradiance and temperature. To extract maximum available power under these changing conditions, a Maximum Power Point Tracking (MPPT) controller continuously measures the PV array's voltage and current and computes the instantaneous power output.Using algorithms such as Perturb-and-Observe or Incremental Conductance, the controller incrementally adjusts the operating voltage and observes the resulting change in power. If power increases, the adjustment continues in the same direction; if it decreases, the controller reverses the adjustment. This process converges on the maximum power point (MPP).Once the MPP is located, the controller modulates the duty cycle of a DC–DC converter—commonly a buck or buck-boost topology—to align the PV array's operating voltage with the battery's charging voltage. The converter steps the PV output up or down as needed while optimizing current flow, ensuring that the solar panels consistently operate at their peak power point. The MPPT charge controller then delivers this regulated output to the battery bank, maximizing charging efficiency. In addition to tracking power, the controller safeguards the batteries by preventing overcharging, deep discharging, and other conditions that could reduce battery life or system reliability.

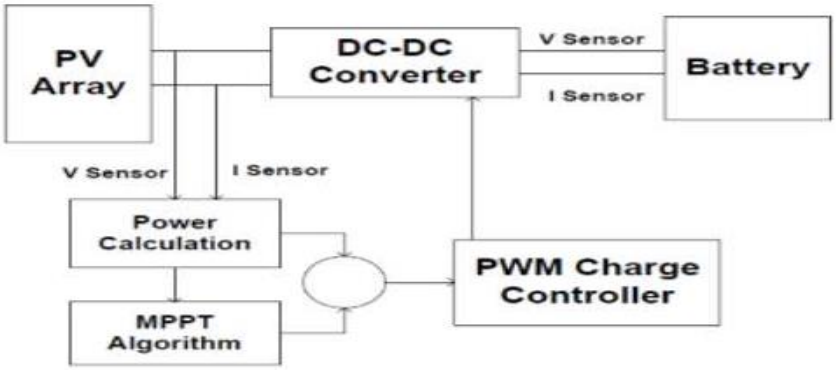

Figure 3.1: Block diagram of an MPPT charge controller

IJIREEICE ISSN (O) 2321-2004, ISSN (P) 2321-5526

International Journal of Innovative Research in Electrical, Electronics, Instrumentation and Control Engineering

Impact Factor 8.021 ⁜ Peer-reviewed & Refereed journal ⁜ Vol. 13, Issue 3, March 2025

DOI: 10.17148/IJIREEICE.2025.13372

3.1 Circuit Diagram

Figure 3.2 provides a detailed circuit diagram representation of the electronic components and their interconnections within the charging system. This includes the AC/DC converter circuit, battery management system, charging control circuitry, sensor connections, and communication module integration with the control unit.

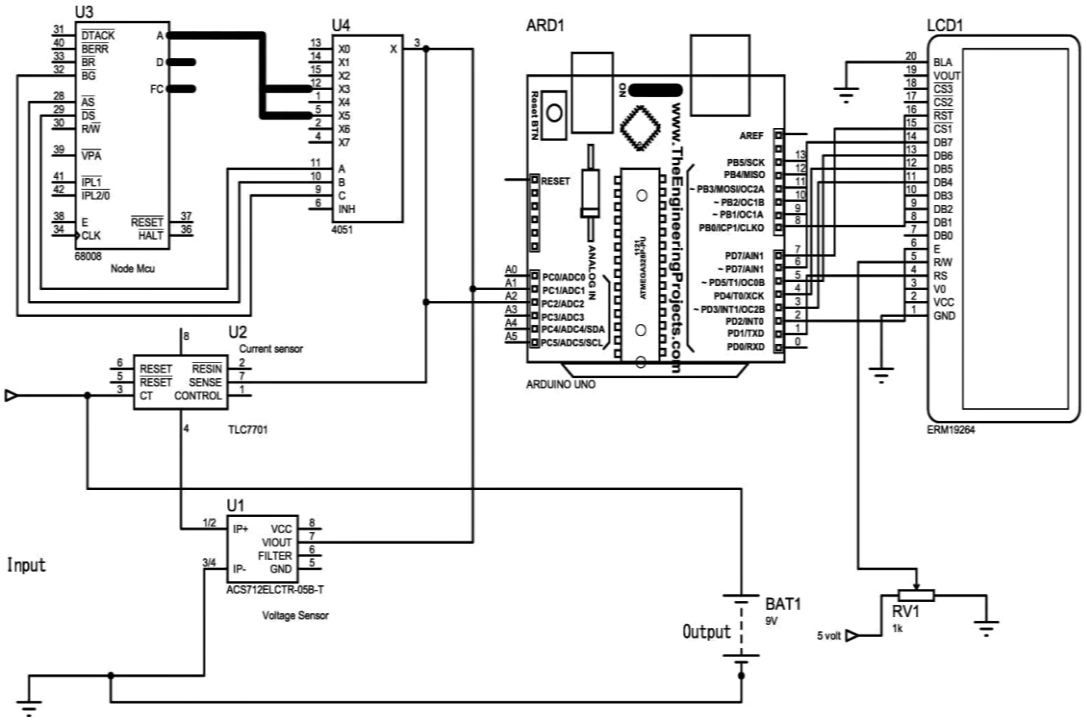

Figure 3.2: Circuit diagram of the Fast Charge Controller

3.2 Design of the DC-DC MPPT Solar Charge Controller

The circuit design of the MPPT solar charge controller is a critical component of its functionality, enabling efficient conversion and management of solar energy. The design incorporates a buck converter topology, utilizing power semiconductor devices, such as metal-oxide-semiconductor field-effect transistors (MOSFETs), which form the core of the energy conversion process. This topology ensures effective regulation of output voltage and current levels. Controlled by the ESP32 microcontroller, the MPPT solar charge controller utilizes the PWM technique for precise control over the duty cycle, facilitating optimal energy extraction from the solar panels. The circuit design can be divided into two primary sections: the control circuit and the power conversion circuit. The control circuit includes components for measuring voltage and current, executing the MPPT algorithm, and managing protection mechanisms. The power conversion circuit focuses on efficiently transforming the solar panel's output into usable charging power for the battery, ensuring stability and reliability throughout the operation.

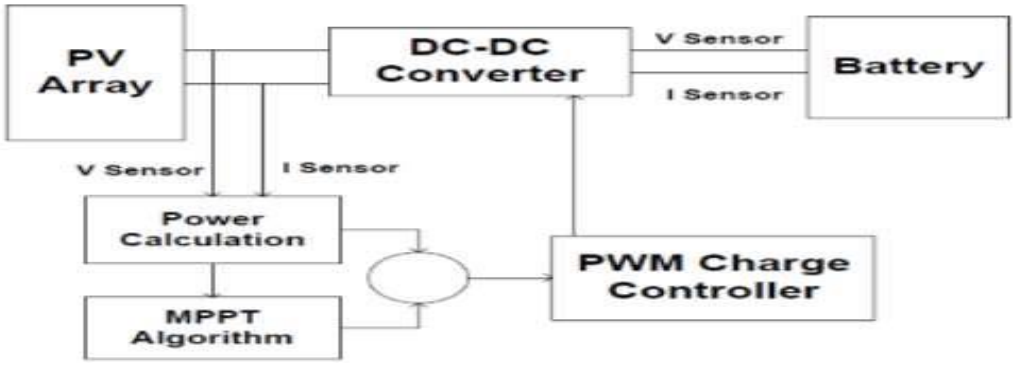

Figure 3.3: Block diagram of an MPPT charge controller

IJIREEICE ISSN (O) 2321-2004, ISSN (P) 2321-5526

International Journal of Innovative Research in Electrical, Electronics, Instrumentation and Control Engineering

Impact Factor 8.021 ⁜ Peer-reviewed & Refereed journal ⁜ Vol. 13, Issue 3, March 2025

DOI: 10.17148/IJIREEICE.2025.13372

Current Sensing: The current sensing mechanism in the MPPT system utilizes the ACS712-30A bidirectional current sensor IC, configured to function as a unidirectional sensor to optimize ADC resolution. The sensor's -IP and +IP pins are connected in reverse, allowing the output voltage (V_{out}) to remain at 2.5V when no current flows. The relationship for current measurement is expressed as:

$$\boldsymbol{V_{out} = 2.5V - (CurrentSensed \times 0.066)} \text{ ---------- (3.1)}$$

This configuration establishes a voltage floor and ceiling that can be scaled to match the ADC's voltage reference, preventing clipping. The focus on refining the current sensing component was driven by past experiences with ACS712 modules, which exhibited significant noise levels. The adjustments made in this design have led to notable improvements in maximum power point (MPP) tracking performance, enhancing the overall efficacy of the MPPT system.

Voltage Sensing: A voltage divider is a common method used to sense and scale down the input voltage to a level suitable for the analogue-to-digital converter (ADC) within the controller. A voltage divider consists of two resistors, R1 and R2, connected in series. The input voltage is applied across the series combination, and the voltage across R2 is measured. The voltage divider equation is:

$$\boldsymbol{V_{out} = V_{in} \times \frac{R2}{R1+R2}} \text{ ---------- (3.2)}$$

Where:

V_{out}: Output voltage (voltage across R2)
V_{in}: Input voltage (voltage from the solar panel)
R1, R2: Resistor values

By carefully selecting the values of R1 and R2, the output voltage can be scaled down to a range that is compatible with the ADC's input voltage range. For example, if the ADC's input voltage range is 0-5V and the maximum expected input voltage from the solar panel is 30V, the voltage divider can be designed to scale down the input voltage to a maximum of 5V. The ADC then converts the analogue output voltage from the voltage divider into a digital value. This digital value can be processed by the controller's microcontroller to determine the input voltage and adjust the buck-boost converter's duty cycle accordingly to track the MPP.

3.3 Main DC-DC Converter Circuitry

The DC-DC buck converter is a vital component in regulating the voltage from the solar panel, stepping it down to match the battery's charging requirements. The ESP32 controls the operation of this converter using a PWM (Pulse Width Modulation) signal to maximize energy transfer.

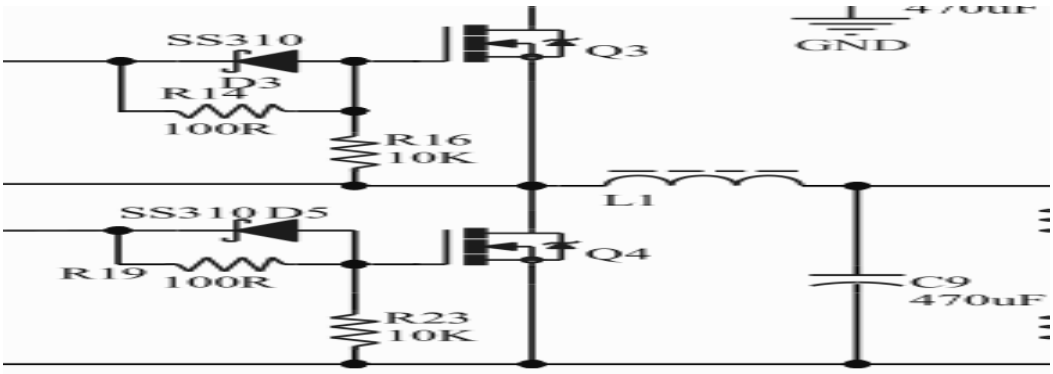

Figure 3.4: Circuit diagram of the main synchronous DC-DC buck converter

In designing a DC-DC buck converter for charge controllers two common designs chosen are either the asynchronous buck converter or the synchronous buck converter. The synchronous converter whilst being more difficult to work with was chosen for use in this work because of its superior efficiency. The synchronous buck converter addresses the inefficiency inherent in the asynchronous buck converter by making a slight but critical modification: replacing the diode with a MOSFET. The diode in an asynchronous buck introduces a significant voltage drop, reducing overall efficiency. A MOSFET, on the other hand, does not experience the same voltage drop when activated, as it operates by applying a

IJIREEICE ISSN (O) 2321-2004, ISSN (P) 2321-5526
International Journal of Innovative Research in Electrical, Electronics, Instrumentation and Control Engineering
Impact Factor 8.021 ⁜ Peer-reviewed & Refereed journal ⁜ Vol. 13, Issue 3, March 2025
DOI: 10.17148/IJIREEICE.2025.13372

voltage between the Gate and Source pins to allow current conduction. MOSFETs function analogously to mechanical switches, with the key advantage of extremely fast switching times, enhancing performance.

3.4 Control Unit

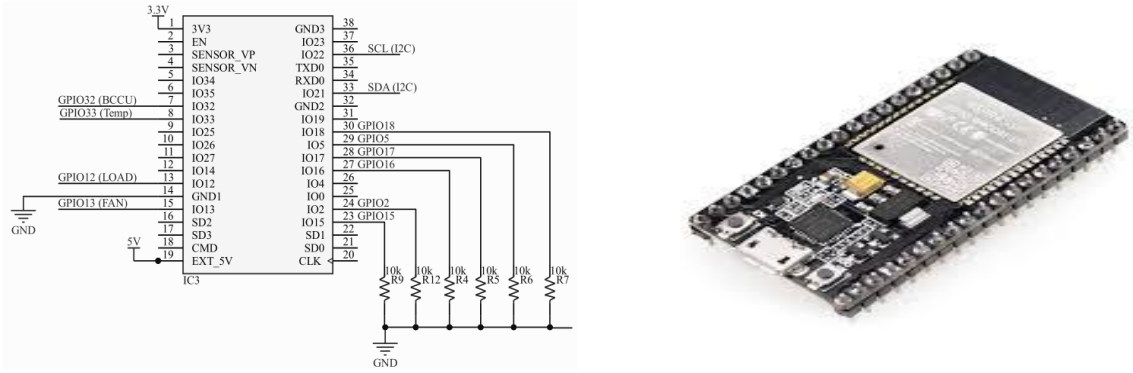

Figure 3.5: Circuit diagram and physical image of the ESP32 microcontroller

The ESP32 (IC3) serves as the central microcontroller in the MPPT system, responsible for managing control, processing, and communication tasks. Several supporting components are integrated to ensure stable and efficient operation. The ESP32 (WROOM32 module) was selected for this project due to its cost-effectiveness and versatility. It is widely available at a low price, yet offers significant advantages, including Arduino compatibility, which simplifies programming and integration into existing systems. The 240 MHz 32-bit dual-core architecture provides the processing power necessary for handling complex algorithms like MPPT. Moreover, the ESP32 comes equipped with built-in Wi-Fi and Bluetooth BLE, eliminating the need for additional wireless communication modules. Its 16-bit PWM resolution allows for precise control of the system's components, particularly in regulating the MOSFETs in the buck converter. Although the ESP32 also features a 12-bit internal ADC, capable of producing 4096 discrete levels for representing voltages and currents, the non-linear behavior of its ADC limits its effectiveness in high-precision applications, leading to less accurate readings in low-voltage ranges.

3.5 Battery Charging and Protection Circuitry

A. **Battery Monitoring**: Effective battery management begins with precise monitoring of both voltage and current. A voltage divider is connected to the battery terminals, enabling the ESP32 to continuously assess the battery voltage. This real-time monitoring allows the charging process to be dynamically adjusted, automatically halting when the battery reaches its full capacity. Additionally, current flowing into the battery is measured using the same current sensor that monitors the solar panel. This data is vital for the controller to maintain charging currents within safe limits, thereby protecting the battery from potential overcurrent conditions.

B. **Overcharge and Over-discharge Protection:** To prevent overcharging, a MOSFET (Q6) is employed as a switch to control the charging process. Once the battery voltage reaches its maximum safe threshold, the ESP32 disables the MOSFET, effectively halting the charging operation and safeguarding the battery against overcharge damage. Furthermore, Schottky diodes (D1 and D4) are integrated to provide reverse current protection. These diodes prevent current from flowing back from the battery to the solar panel during periods of insufficient sunlight, ensuring that no energy is wasted and that the battery is protected from unnecessary discharge.

C. Backflow Current Control Unit (BCCU): The Backflow Current Control Unit (BCCU) is designed to prevent reverse current from entering the system, which could potentially damage components and decrease system efficiency. This unit plays a crucial role in managing current flow, ensuring that the circuit remains protected from undesired backflow. The operation of the BCCU is controlled through GPIO32: When GPIO32 is set to HIGH, Q1 conducts, providing power to the relay from the 12V line. This action enables the isolated 12V supply to turn the relay on, allowing current to flow. When GPIO32 is set to LOW, power is cut off from Q1 and therefore the relay, and R13 safely discharges any remaining charge at the gate of Q1, ensuring it turns off and prevents reverse current from flowing.

D. Temperature Monitoring: A temperature sensor is incorporated into the system to monitor the temperature of the MOSFETs (Q3 and Q4). The ESP32 utilizes this information to regulate the speed of the included fan and ensure the MOSFETs do not overheat at high current draw. This also helps to ensure the thermal stability of the charger especially during the charging process.

IJIREEICE ISSN (O) 2321-2004, ISSN (P) 2321-5526

International Journal of Innovative Research in Electrical, Electronics, Instrumentation and Control Engineering

Impact Factor 8.021 ⁜ Peer-reviewed & Refereed journal ⁜ Vol. 13, Issue 3, March 2025

DOI: 10.17148/IJIREEICE.2025.13372

3.6 MPPT Algorithm Implementation

The MPPT (Maximum Power Point Tracking) algorithm is central to the controller's ability to optimize energy extraction from the solar panel. The specific algorithm chosen for this project is the Perturb and Observe (P&O) method. The Perturb and Observe (P&O) algorithm is a fundamental approach utilized within the MPPT control system to ensure optimal energy extraction from the solar panel. The operational sequence of the P&O algorithm is as follows:
Initially, the system measures the voltage and current output of the solar panel. From these values, the power is calculated using the formula:

$$\boldsymbol{P = V \times I}$$ ---------- (3.3) Where, P = Power V = Voltage I = Current

Subsequently, the ESP32 makes slight adjustments, or perturbations, to the duty cycle of the buck converter's PWM signal and monitors any resulting changes in power output. If an increase in power is observed, the perturbation continues in the same direction conversely, if power decreases, the perturbation direction is reversed. This iterative process allows the controller to continuously track the maximum power point (MPP) of the solar panel, adapting to changing sunlight conditions.

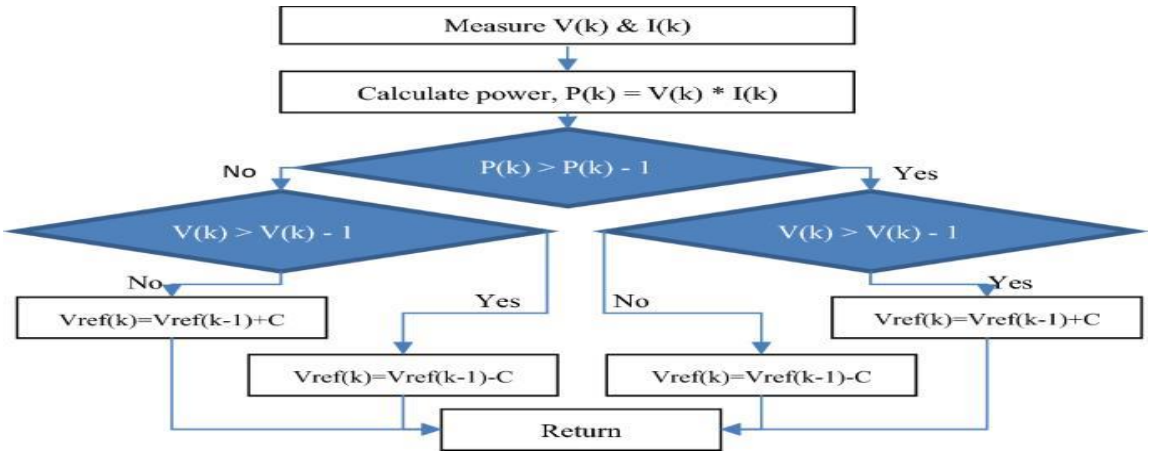

Figure 3.6: P & O algorithm flowchart

Where,
V(k) is the current value of PV output voltage, V(k) − 1 is the previous value of the PV output voltage
I(k) is the current value of the PV current, P(k) is the current value of the PV output power
P(k) − 1 is the previous value of the PV output power, Vref is reference output voltage of the P&O controller. By employing this algorithm, the system maximizes energy extraction, thus enhancing overall efficiency and performance.
In the design of the MPPT system, it is crucial to establish a specific floor value for the PWM duty cycle. The PWM floor duty cycle can be calculated using the formula:

$$\boldsymbol{PWMFloorDutyCycle = \frac{V_{out}}{V_{input}} \times 100}$$ ---------- - (3.4)

Where, V_{out} = Output Voltage, V_{in} = Input Voltage
This formula determines the minimum permissible duty cycle based on the output voltage of the system in relation to the input voltage. The derived PWM floor duty cycle represents the ideal unloaded PWM duty cycle needed for the buck converter to output a voltage that matches the battery voltage. The resolution and frequency of the PWM signal are vital parameters that significantly impact the performance of the MPPT's buck converter. A higher PWM resolution results in finer voltage and current steps at the output, enhancing the accuracy of the regulation. Conversely, a lower PWM resolution yields coarser steps, which can lead to less precise control. Moreover, increasing the PWM frequency improves the power handling capability of the buck converter and reduces output ripple. However, this adjustment must be made judiciously; while higher frequencies may enhance power handling, they also increase switching losses to a certain extent. A relationship exists between PWM resolution and frequency, defined by the following formula:

$$\boldsymbol{MaxPWMFrequency = \frac{MCUClock}{PWMResolution}}$$ ---------- (3.5)

IJIREEICE ISSN (O) 2321-2004, ISSN (P) 2321-5526

International Journal of Innovative Research in Electrical, Electronics, Instrumentation and Control Engineering

Impact Factor 8.021 ⁜ Peer-reviewed & Refereed journal ⁜ Vol. 13, Issue 3, March 2025

DOI: 10.17148/IJIREEICE.2025.13372

IV. SYSTEM IMPLEMENTATION

These components were developed and tested independently. The software was also developed and tested. After they had produced the expected results, they were combined to form the charging system. The following expected Outcomes are expected from the developed system.

- Optimized Fast-Charging Infrastructure: A system capable of rapidly charging batteries in swap stations, reducing vehicle downtime and enhancing user convenience.
- Enhanced Battery Safety and Longevity: Implementation of thermal management and optimized charging protocols to maintain battery integrity over extended use.
- Scalable Design Framework: A modular system design that can be adapted for various battery types and station capacities, facilitating widespread adoption.

4.1 Implementation of the DC-DC converter circuitry

A test for the workability of the components used in the sections of the DC-DC converter was carried out as like those of the control circuit. For the switching section, a test of the MOSFETs working condition was carried out. A test for the MOSFET pins was done by the use of multi-meter to test for the gate, source and drain pin. This was done by setting the multi-meter to the diode mode. The black probe of the meter is connected to the source and the red probe to the drain of the device. An open circuit indication on the meter confirms that the MOSFETs were in good working condition. In construction, A bulk capacitor, designed to filter out ripple voltages caused by the fast-switching nature of the buck converter, thus ensuring stable voltage regulation is connected across the output terminals of the converter circuit. Pull-down resistors are included to prevent MOSFET Q3 from floating before start-up, ensuring that the MOSFET remains in the off state until properly triggered, and thereby maintaining stable operation. Gate resistors are also included that limit transient currents provided by the IR2014 (IC2), protecting the gate pins of Q3 and Q4 from potentially damaging surges during switching. Schottky diodes are added to offer a quick return path for discharging the gate charges of Q3 and Q4, allowing the MOSFETs to turn off rapidly and efficiently, contributing to the overall switching performance. A bootstrap capacitor is utilized by IC2's charge pump to supply the necessary power for the high-side N-channel MOSFET (Q3), ensuring proper switching action. Also a fan is used reduce the temperature of the MOSFETs during periods of prolonged usage at high currents. Additional tests were carried across the following sectors:

- **Voltage Regulation**: The buck converter effectively regulated the output voltage to meet the battery's charging requirements, maintaining a stable output of 52V to 72V for a 72V lithium-ion battery. The ESP32's PWM control over the MOSFET allowed precise adjustment of the voltage in response to changing solar input.
- **Current Regulation:** The current supplied to the battery was also well-regulated. Through the use of the current sensor and the external ADC, the system maintained safe current levels, preventing over-current situations. The charging current typically ranged from 24A to 40A, depending on the available sunlight.
- **Overall Efficiency:** The overall efficiency of the DC-DC converter was measured to be between 87% and 96%, with minor losses due to switching and heat dissipation. This high efficiency contributed to the system's ability to manage energy conversion effectively.

4.2 Implementation of the Input monitoring and power delivery circuitry

Given the components and functionality of the charge controller, the following tests were conducted on its input and power delivery section: A wide range of input voltages within the controller's specified range were tested and it was verified that the voltage divider accurately reflects the input voltage to the micro controller. The ACS712 current sensor was tested across the full range of expected currents to verify its accuracy using a variable DC power supply and a multi-meter. The sensor's sensitivity to noise and its stability over time was also tested.

Table 4.1: ACS712-30A (Current & Output Voltage Relationship)

Current (A)	Analog Output Voltage (V)
-35	0.19
-30	0.52
-25	0.85
-20	1.18
-15	1.51

IJIREEICE ISSN (O) 2321-2004, ISSN (P) 2321-5526

International Journal of Innovative Research in Electrical, Electronics, Instrumentation and Control Engineering

Impact Factor 8.021 ⁜ Peer-reviewed & Refereed journal ⁜ Vol. 13, Issue 3, March 2025

DOI: 10.17148/IJIREEICE.2025.13372

-10	1.84
-5	2.17
0	2.5
5	2.83
10	3.16
15	3.49
20	3.82
25	4.15
30	4.48
35	4.81

4.3 Implementation of Software and firmware development

The PWM floor value should never drop to 0% or below when a battery is connected to the output. Should the PWM signal drop below this computed threshold, the consequence is a potential reversal of current flow, causing MOSFET Q4 to conduct unexpectedly, This results in the battery discharging instead of charging, leading to undesirable operational states. To mitigate this issue, the firmware implements a control mechanism where the SD pin of the IR2104 is set to LOW when the PWM falls below the computed floor limit. This ensures that both Q3 and Q4 remain off during such states, thereby preventing any unintended conduction. This approach constrains the maximum allowable PWM duty cycle since charge pump MOSFET drivers, such as the IR2104, cannot operate at 100% duty cycle due to design limitations. The constrain function in the Arduino programming environment is utilized to ensure that the PWM signal does not exceed the defined ceiling limit or fall below the floor limit. Concerning the PWM resolution and frequency in (3.8), given that the MCU clock of the ESP32 operates at 80MHz, one can select either PWM frequency or resolution as the variable of interest. After evaluating various configurations for PWM resolution and frequency, the optimal settings established for the MPPT design and firmware were 11-bit resolution at a frequency of 39 kHz. This configuration provided a balance between stability and responsiveness, ensuring adequate switching frequency while minimizing power loss. The firmware includes comments that highlight adjustable variables for modifying PWM resolution and frequency as needed. The firmware also includes variables for the panel and battery specifications which are all configured to be controllable from the LCD using the included buttons.

Table 4.2: Esp32: PWM resolution & PWM frequency table

Resolution (Bits)	**Resolution (decimal)**	**Max PWM Frequency (kHz)**
1	2	40000
2	4	20000
3	8	10000
4	16	5000
5	32	2500
6	64	1250
7	128	625
8	256	312.5
9	512	156.25
10	1024	78.125
11	2048	39.0625
12	4096	19.53125

IJIREEICE ISSN (O) 2321-2004, ISSN (P) 2321-5526

International Journal of Innovative Research in Electrical, Electronics, Instrumentation and Control Engineering

Impact Factor 8.021 ⁜ Peer-reviewed & Refereed journal ⁜ Vol. 13, Issue 3, March 2025

DOI: 10.17148/IJIREEICE.2025.13372

4.4 Implementation of the battery charging and Protection circuitry

The NTC heat sensor was employed to measure temperature of the synchronous buck converter MOSFETs. Before connecting it to the micro-controller. it was tested to ensure its reliability. The NTC sensor was tested by simply measuring the resistance value of the NTC with a meter. A good reading from the meter indicated that the sensor was in a good working condition. The relay was also tested prior to connecting with the controller. A multi-meter was used to carry out the test, which includes measuring the resistance value of the relay's pins. For a 12V relay which was utilized in this project, the coil resistance value as stated by the manufacturer is around 320 ohms. When the test was completed, the coil resistance measured 280 ohms. This is a high value, indicating that the relay coil is good. The relay's other terminals were also tested by measuring the resistance between the terminals. For a NO terminal, the resistance value should read high indicating an open circuit while for NC terminal, the resistance value should read approximately zero; indicating a closed circuit. Following confirmation that all the components were suitable and good for use; they were connected to the micro controller.

4.5 Simulation Results

To simulate the behavior and performance of the charge controller, Proteus Design software was used to create a detailed model of the circuit, including the solar panel, battery, buck-boost converter, and other relevant components. Accurate models for these components were obtained or created, and realistic input signals representing solar irradiance and temperature variations were generated. Once the model was constructed and parameters were defined, the simulation was run to observe the controller's response to the input signals. Data on the controller's output voltage, current, power, and other relevant parameters were collected and analyzed to evaluate the MPPT algorithm's performance, efficiency, battery charging capability, and transient response. Sensitivity analysis was conducted by varying key parameters to assess their impact on the controller's performance. This provided valuable insights for design optimization and troubleshooting.

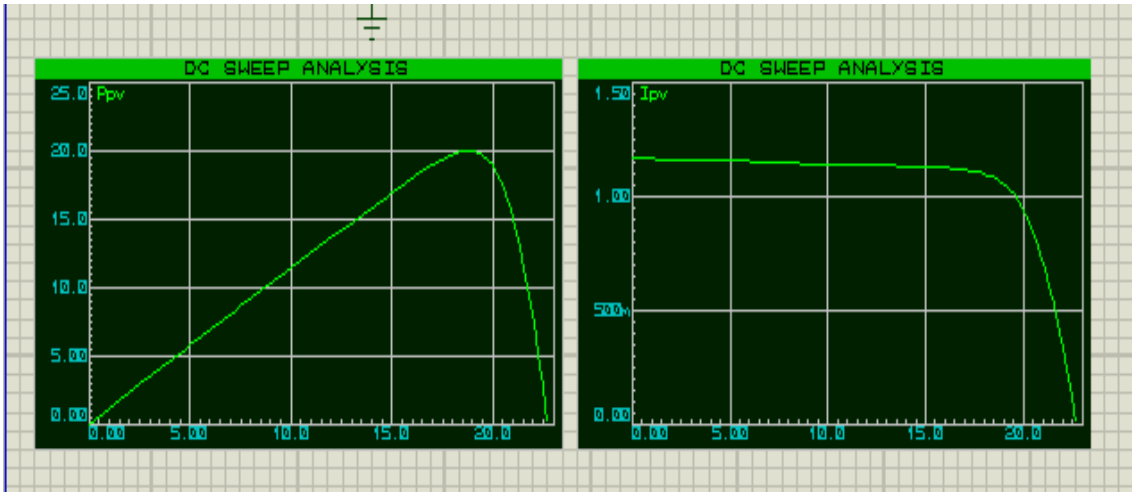

Figure 4.1: DC sweep analysis for output voltage and current as system approaches MPP

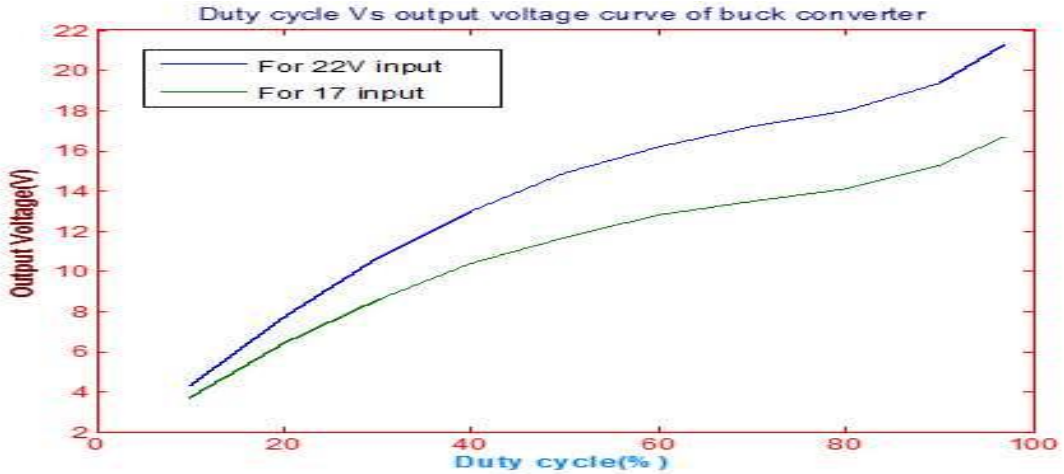

Figure 4.2: Duty cycle variations of the main DC-DC buck converter for different outputs

IJIREEICE ISSN (O) 2321-2004, ISSN (P) 2321-5526

International Journal of Innovative Research in Electrical, Electronics, Instrumentation and Control Engineering

Impact Factor 8.021 ⁜ Peer-reviewed & Refereed journal ⁜ Vol. 13, Issue 3, March 2025

DOI: 10.17148/IJIREEICE.2025.13372

4.6 Testing of the System

To evaluate the performance and reliability of the charge controller, a comprehensive testing procedure was conducted. By applying varying input voltages and monitoring the controller's output, its ability to operate effectively in different sunlight conditions was determined. Efficiency was measured by comparing the input and output power. The controller's battery charging performance was tested with different battery types to ensure compatibility and safe charging. Temperature stability was assessed by subjecting the controller to varying temperatures and monitoring its performance.

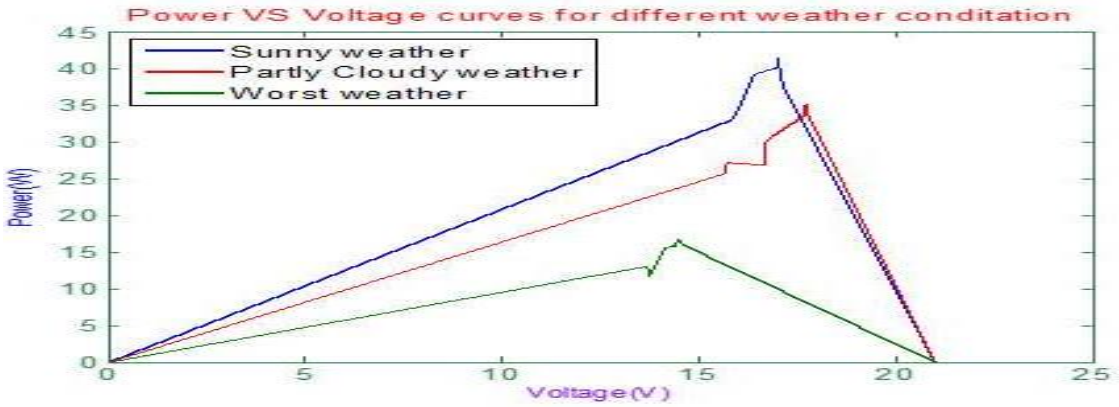

Figure 4.3: Output power against different output voltages in various weather conditions

4.7 Packaging

The implemented system was packaged to create a visually appealing device. Several aspects were considered for packaging including the longevity of the material utilized. Plastic Perspex casing was chosen for this project due to its low cost, easy workability and non-conducting nature. The package's portability was considered in order to restrict the amount of space it will take up and to reduce the strain associated with device relocation.

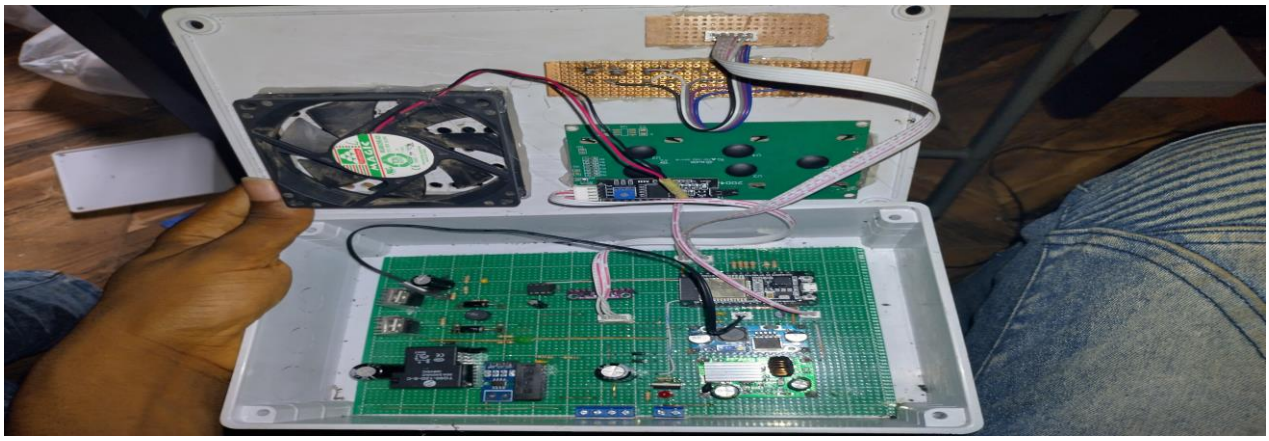

Figure 4.5: The packaging of the fast Charge controller

V. CONCLUSION

This research aims to advance the functionality and efficiency of battery swap stations by developing a fast-charging system that addresses critical aspects such as charging speed, thermal management, and battery health. The successful implementation of this system could significantly enhance the practicality of battery swapping as a viable solution for EV energy replenishment. By utilizing clean energy sources such as solar power, the charge/swap station not only reduces dependence on fossil fuels but also contributes to environmental conservation efforts. Overall, this study reveals the importance of innovative solutions in addressing the challenges of sustainable urban transportation. The successful implementation of the fast charger solution for the smart-solar powered charge/swap station for E-Rickshaws serves as a testament to the efficacy of collaborative efforts between academia, industry, and technology providers in driving positive change towards a greener and more sustainable future as well as aid gain sustainable traction for the utilization of E-Rickshaws as the most convenient and sustainable means of public transportation.

DOI: 10.17148/IJIREEICE.2025.13372

REFERENCES

[1]. Administrator. (n.d.). Daily Generation. Retrieved from http://www.bpdb.gov.bd/bpdb/index.php?option=com_content&view=article&id=20&Itemid

[2]. All-battery. (2019). battery. Retrieved from http://www.all-battery.com/12V20AHLP12-20Maintenance-freeSealedLeadAcidSLABattery-40806.aspx

[3]. Arya, H., & Das, M. (2023). Fast Charging Station for Electric Vehicles Based on DC Microgrid. IEEE Journal of Emerging and Selected Topics in Industrial Electronics, 1–8. https://doi.org/10.1109/jestie.2023.3285535

[4]. Assadi, S. A., Gong, Z., Coelho, N., Zaman, M. S., & Trescases, O. (2023). Modular Multiport Electric-Vehicle DC Fast-Charge Station Assisted by a Dynamically Reconfigurable Stationary Battery. IEEE Transactions on Power Electronics, 38, 6212–6223. https://doi.org/10.1109/TPEL.2023.3237622

[5]. Ayyadi, S., Ahsan, S. M., Khan, H. A., & Arif, S. M. (2024). Optimized Energy Management System for Cost-effective Solar and Storage Integrated Fast-Charging Station. 1–5. https://doi.org/10.1109/isgt59692.2024.10454210

[6]. Basu, A., & Singh, M. (2023). Performance analysis of PV based battery integrated e-rickshaw with regenerative braking. Microsystem Technologies, 1-11.

[7]. Battery University. (n.d.). Charging Information For Lead Acid Batteries. Retrieved from https://batteryuniversity.com/index.php/learn/article/charging_the_lead_acid_battery

[8]. Control and Application Research Centre (CARC), BRAC University. (2014). Power Conservation for Electrically Assisted Rickshaws with PV Support, Torque Sensor Paddle, and the Solar Battery Charging Station – A Complete Solution [Technical report].

[9]. Dhaka Transport Co-ordination Board. (2005). Strategic Transport Plan for Dhaka- Final Report. Dhaka, Bangladesh.

[10]. Dhar, S., Jayakumar, A., Lavanya, R., & Kumar, M. D. (2021). Techno-economic assessment of various motors for three-wheeler E-auto rickshaw: From Indian context. Materials Today: Proceedings, 45, 6572-6579.

[11]. Draz, A.-S. E., Othman, A. M., & El-Fergany, A. A. (2023). State-of-the-Art with Numerical Analysis on Electric Fast Charging Stations: Infrastructures, Standards, Techniques, and Challenges. Renewable Energy Focus. https://doi.org/10.1016/j.ref.2023.100499

[12]. Gallagher, R. (1992). The Rickshaws of Bangladesh. Dhaka, Bangladesh: University Press Ltd.

[13]. Gupta, J., Singh, B., & Kushwaha, R. (2020, December). A Rooftop Solar PV Assisted On-Board Enhanced Power Quality Charging System for E-Rickshaw. In 2020 International Conference on Power, Instrumentation, Control and Computing (PICC) (pp. 1-6). IEEE.

[14]. Hadjilambrinos, C. (2021). Reexamining the automobile's past: What were the critical factors that determined the emergence of the internal combustion engine as the dominant automotive technology?. Bulletin of Science, Technology & Society, 41(2-3), 58-71.

[15]. Haldar, I., Debnath, D., & Choudhury, T. R. (2021, January). Design of a battery charger fed from two solar panels arranged at different inclination for e-rickshaw and dc microgrid applications. In 2021 1st International Conference on Power Electronics and Energy (ICPEE) (pp. 1-6). IEEE.

[16]. Hasan, A. M. (2020). Electric rickshaw charging stations as distributed energy storages for integrating intermittent renewable energy sources: a case of Bangladesh. Energies, 13(22), 6119.

[17]. https://www.futurehome.io/en/can-extreme-fast-charging-of-a-lithium-ion-battery-extend-its-lifespan. Accessed on 5th March, 2025.

[18]. https://clouglobal.com/the-future-of-electric-vehicle-charging-fast-furious-and-fossil-fuel-free/ Accessed on 5th March, 2025.

[19]. Khaligh, A., & Onar, O.C. (2010). Energy Harvesting-Solar, Wind, and Ocean Energy Conversion Systems. CRC Press.

[20]. Mithu, K., Hauqe, E., & Hasan, M. S. (2017). Design of a Micro-Controller Based Charge Controller for Electric Rickshaw. Doctoral dissertation, Department of Electrical, Electronic and Communication Engineering. Retrieved from http://hdl.handle.net/123456789/419

[21]. Modern Survival Blog. (2019). Charging battery. Retrieved from http://modernsurvivalblog.com/alternative-energy/battery-state-of-charge-chart.

[22]. Mulhall, P., Lukic, S.M., Wirasingha, S.G., Lee, Y.J., & Emadi, A. (2010). Solar-Assisted Electric Auto Rickshaw Three-Wheeler. IEEE Transactions on Vehicular Technology, 59(5), 2298-2307.

[23]. Nadimuthu, L. P. R., & Victor, K. (2021). Performance analysis and optimization of solar-powered E-rickshaw for environmental sustainability in rural transportation. Environmental Science and Pollution Research, 28, 34278-34289.

[24]. Narasipuram, R. P., & Mopidevi, S. (2021). A technological overview & design considerations for developing electric vehicle charging stations. Journal of Energy Storage, 43, 103225.

DOI: 10.17148/IJIREEICE.2025.13372

[25]. Northern Arizona Wind & Sun. (n.d.). Solar Charge Controller Basics. Retrieved from https://www.solar-electric.com/solar-charge-controller-basics.html

[26]. Priye, S., Manoj, M., & Ranjan, R. (2021). Understanding the socioeconomic characteristics of paratransit drivers and their perceptions toward electric three-wheeled rickshaws in Delhi, India. IATSS research, 45(3), 357-370.

[27]. Rajendran, G., Vaithilingam, C. A., Misron, N., Naidu, K., & Ahmed, M. R. (2021). A comprehensive review on system architecture and international standards for electric vehicle charging stations. Journal of Energy Storage, 42, 103099.

[28]. Ray, O., Rana, M. S., Mishra, S., Davies, K., & Sepasi, S. (2020, December). Battery-swap Technology for e-Rickshaws: Challenges, Opportunity and Scope. In 2020 21st National Power Systems Conference (NPSC) (pp. 1-6). IEEE.

[29]. Renewable Energy Resource Centre (RERC), University of Dhaka. (2007). Final Report of Solar and Wind Energy Resource Assessment (SWERA) – Bangladesh Project.

[30]. Richard, L., & Petit, M. (2018). Fast charging station with battery storage system for EV: Grid services and battery degradation. IEEE International Energy Conference, 1–6. https://doi.org/10.1109/ENERGYCON.2018.8398744

[31]. Roy, A. (2016). E-rickshaw service in Barddhaman town: importance, problems and future prospects. International journal of Scientific and Research Publication, 6(9), 702-706.

[32]. Shankar, D., Biswas, M., & Datta, R. (2021). Design of Low-Cost Solar Powered E-Rickshaw: A Case Study. In Proceedings of International Conference on Thermofluids: KIIT Thermo 2020 (pp. 561-568). Springer Singapore.

[33]. Singh, S., Mathur, A., Das, S., Sinha, P., & Singh, V. (2017). Development of Smart PublicTransport System by Converting the Existing Conventional Vehicles to EV's in Indian Smart Cities (No. 2017-01-2011). SAE Technical Paper.

[34]. Singh, S., Mathur, A., Das, S., Sinha, P., & Singh, V. (2017). Development of Smart PublicTransport System by Converting the Existing Conventional Vehicles to EV's in Indian Smart Cities (No. 2017-01-2011). SAE Technical Paper.

[35]. Verma, A. D., Shishodia, V., Tomar, A., & Gaur, P. (2023, February). Commercial Solar PV Off-Grid Battery Charging/Swapping Station: Opportunity and Solution for E-rickshaw. In 2023 2nd Edition of IEEE Delhi Section Flagship Conference (DELCON) (pp. 1-7). IEEE.

[36]. Wakefield, E. H. (1993). History of the electric automobile: battery-only powered cars. SAE International.

[37]. Yilmaz, M., & Krein, P. T. (2012). Review of battery charger topologies, charging power levels, and infrastructure for plug-in electric and hybrid vehicles. IEEE transactions on Power Electronics, 28(5), 2151-2169.]. Electrical World and Engineer, 2011. URL: http://www.tfcbooks.com/tesla/1904-03-05.htm Accessed 10, November 2019.